16th World Conference on Earthquake, 16WCEE 2017

Santiago Chile, January 9th to 13th 2017

Paper N° 75

Registration Code: S-C1450662207

Out-of-plane Dynamic Test of Unreinforced Masonry Walls Retrofitted and Response Values of Recent Acceleration Records

M. Inukai[(1)], T. Azuhata[(2)], K. Morita[(3)], K. Noguchi[(4)],M. Tani[(5)]

[(1)] *Chief Research Engineer, International Institute of Seismology and Earthquake Engineering (IISEE), Building Research Institute (BRI), inkm@kenken.go.jp*
[(2)] *Chief Research Engineer, IISEE, BRI, azuhata@kenken.go.jp*
[(3)] *Head, Building Department, National Institute for Land and Infrastructure Management (NILIM), morita-k92ha@nilim.go.jp*
[(4)] *Chief Official, Head Officer for General Affairs, NILIM, noguchi-k92hu@nilim.go.jp*
[(5)] *Associate Professor, Kyoto University Graduate School, tani@archi.kyoto-u.ac.jp*

Abstract

This paper describes the out-of-plane dynamic test results of unreinforced masonry walls in the Section 1 and the response values of acceleration records in recent years in the Section 2.

In the Section 1, the houses of unreinforced masonry walls are used in the developing countries. They sometime collapsed in the direction of out-of-plane in severe earthquakes. The retrofitting and the disaster reduction of them are necessary.

Therefore, the out-of-plane dynamic tests of unreinforced masonry walls are executed to know the effects of retrofitting.

The specimen has 3 walls, which are a main wall and the 2 transverse walls. The 1st specimen is considered to be a 1st storey house, and the 2nd specimen is to be the 1st storey of the 2 storey house. Both specimens are retrofitted by the popular wire netting on one side of in-house.

The predominant frequency of the masonry walls with retrofitting are near to the frequency of the natural period of the specimen or the predominant frequency on the steel frame basement.

The damping factors are also calculated. They are from 2% to 5%.

In the Section 2, the response values of acceleration records of 2016 Kumamoto Earthquake and 2015 Kathmandu Earthquake are analyzed. These response values are caparisoned with those of the recent acceleration records.

Keywords: Unreinforced Masonry Wall; Out-of-plane; Retrofit; Damping Factor; Shear Coefficient

1. Out-of-plane Dynamic Test of Unreinforced Masonry Walls Retrofitted

1.1 Introduction

The houses of unreinforced masonry walls are used in the developing countries. They sometime collapsed in the direction of out-of-plane in severe earthquakes. The retrofitting and the disaster reduction of them are necessary. Therefore, the out-of-plane dynamic tests of unreinforced masonry walls are executed to know the behaviors of the wall specimen and the wall with a floor specimen.

1.2 Specimens

The specimen has 3 walls, which are a main wall and the 2 transverse walls. The 1st specimen is considered to be a 1st storey house, and the 2nd specimen is to be the 1st storey of the 2 storey house. Both specimens are retrofitted by the popular wire netting on one side of in-house (Fig. 1). The dimensions of the unit (brick popular on sale) is length 210 × width 100 × height 60mm. The joint thickness is 10mm and the wall thickness is a half (= 100mm). The specimens are built up on the steel frame foundation. The dimensions of the central wall of the 3 walls of the specimens are 1390 height × 2850 length × 100mm thickness. The dimensions on both sides of the transverse wall, is 1390 height × 1420 length × 100mm thickness. Joint mortar is produced by the mixture ratio (weight ratio of cement to sand) 1:5. After the wall specimens production, the air curing period was one month. The wire netting (hexagonal wire mesh, wire diameter 1.0mm, mesh size 26mm) was anchored on the inside the entire surface of the wall in the vertical joints. At the time of the anchor, the U-shaped staples, about 240mm spacing, were used for the wire netting on the wall (Photo 2). In the horizontal joints, it has no anchors. When the specimens are moved to the shaking table, they are lifted with the steel frame foundation. After fixing the steel frame foundation to shaking table, the wooden floor and a steel weight are put on the walls,. The sum of the weight of the wooden floor and the steel weight is 18kN.

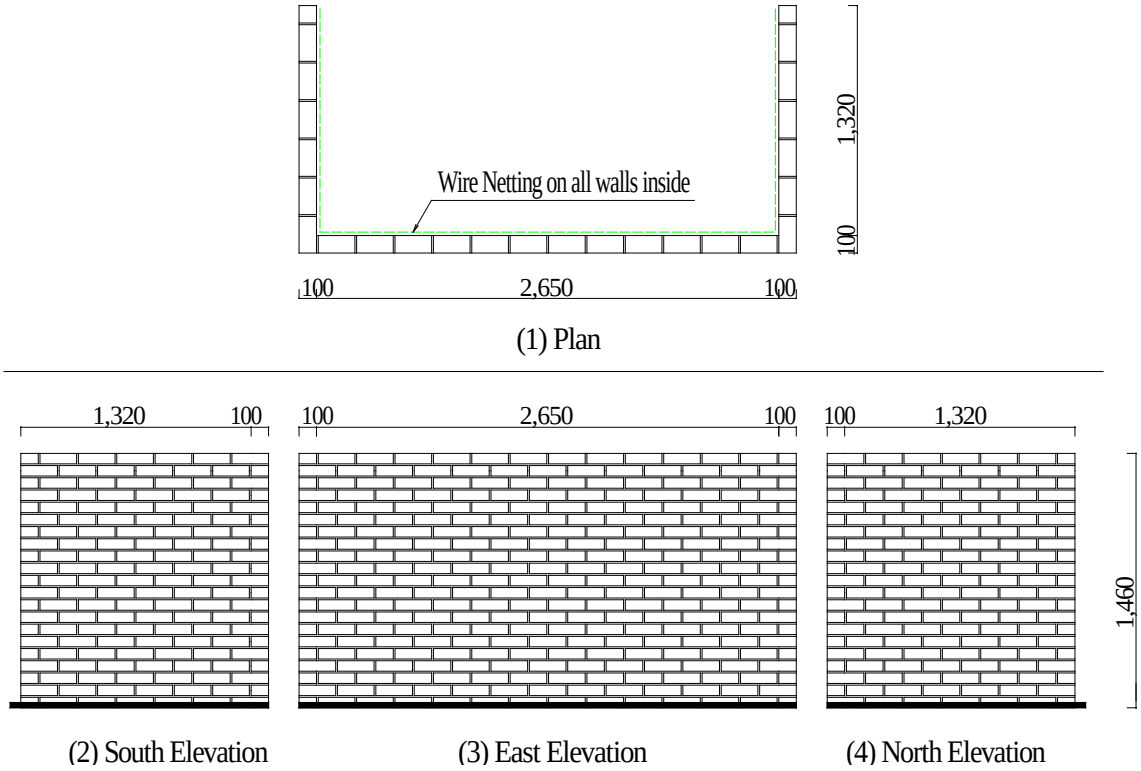

Fig. 1 – Specimen (Wall with wire netting without Floor)

(1)Wall without Floor (2)Wall with Floor

Photo. 1 – Specimens (After wire netting before Test)

(1)Wall without Floor (2)Wall before with Floor working

Photo. 2 – Details of wire netting in Specimens

1.3 Test Results

1.3.1 Material Test Results

In material tests, the compression test pieces are the half thickness and 3 layers (height 200 × length 210 ×thickness 100mm) which are 3 test pieces. The diagonal compression test pieces are half thickness and 4 layers (270 × 270mm) which are 3 test pieces. The average values in the wall without floor, 17.2MPa, 6.08MPa, and in the wall with floor 11.2MPa, was 4.15MPa.

1.3.2 Out-of-plane Dynamic Test of Unreinforced Masonry Walls Retrofitted

Shaking table tests, in September 2013 and September 2014, were conducted at the medium-sized shaking table in the Structure Laboratory, Building Research Institute. The loading direction is one horizontal direction (east-west direction), by changing the frequency and the amplitude were swept or random waves (Table 1, Table 2). On the wall without floor specimen, the waves of 25%, 50% and 70% of the acceleration amplitude of 1995JMA-Kobe-NS was also carried out. Three sides of the outside the specimens and on the steel frame foundation, the 16 single-axis type accelerometer and the 7 PI-gauges instrumented. These measuring directions are the vibration direction (east-west direction), the transverse direction (north-south direction) or up-and-down direction of the acceleration, and vertical joint or by measuring the joint width of the horizontal joint (Fig. 2, Fig. 4). Measurement, using a dynamic strain meter, was measured simultaneously.

According to the experimental results, the peak of the shaking test waves and measured acceleration, are shown in Table 1, Table 2.

Table 1 – Shaking Test Waves and Peaks of Measured Acceleration of Wall Specimen with Wire Netting without Floor

Shaking Test Waves (Shaking to 1 direction in horizontal and out-of-plane of the Central Wall)				Measured Acceleration (Shaking Direction)		
				Peak at	Peak at the Central Wall	
No.	Wave Type	Frequency (Hz)	Amp. (mm)	Steel Frame Foundation (g)	Upper and Center (g)	Middle and Center (g)
1	Sweep	0.8 - 20	0.5	0.18	1.99	1.50
2	Random	5 - 20	0.5	0.02	0.11	0.07
3	Random	10 - 15	0.5	0.02	0.07	0.05
4	Random	10 - 15	2	0.05	0.24	0.17
5	Random	10 - 15	5	0.12	0.60	0.44
6	Random	10 - 15	10	0.29	2.25	1.60
7	Random	10 - 15	15	0.34	2.65	1.78
8	Random	5 - 15	5	0.15	0.73	0.62
9	Random	5 - 15	10	0.34	1.81	1.47
10	Random	5 - 15	15	0.50	2.75	2.00
11	Random	5 - 15	20	0.65	3.68	2.17
12	Random	5 - 15	25	0.91	3.46	2.53
13	Random	5 - 15	30	1.14	4.56	2.64
14	Random	5 - 15	35	1.15	4.96	2.71
15	Random	5 - 15	40	1.36	4.97	3.01
16	Random	5 - 15	45	1.50	5.01	2.87
17	Random	5 - 15	50	1.55	2.39	3.84
18	Random	5 - 15	55	1.85	3.50	4.01
19	Random	5 - 15	60	2.06	2.90	4.38
20	Kobe_25%			0.26	0.48	0.29
21	Kobe_50%			0.50	1.34	0.53
22	Kobe_70%			0.69	－(*1)	0.91
23	Random	5 - 15	70	2.22	－(*2)	0.34

Notes) (*1): During shaking, masonry brick units, with acclerometers, fell down.
(*2): Measuring impossible.

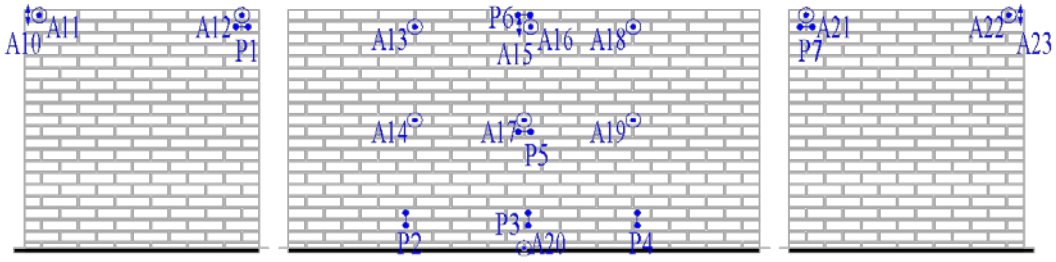

(1)South Elevation (2)East Elevation (3)North Elevation

(Note) : Accelerometers in the direction of out-of- plane
: Accelerometers in the direction of vertical
: PI gauges

Fig.2 –Instrumentation for the test (Wall without Floor)

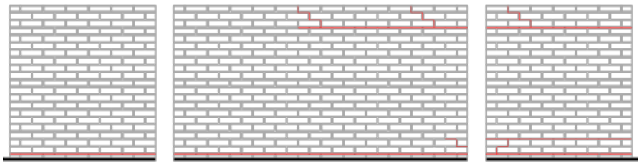

(i)South Elevation (ii)East Elevation (iii)North Elevation

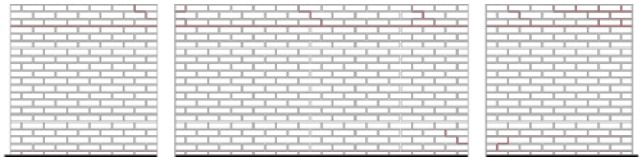

(i)South (ii)East (iii)North

(1) After 15th Wave (2) After 17th Wave

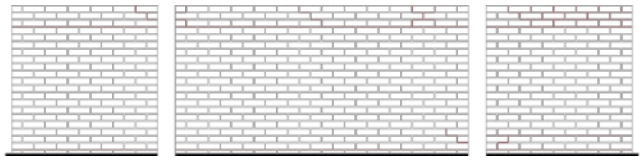

(i)South (ii)East (iii)North

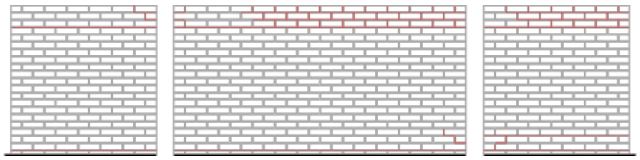

(i)South (ii)East (iii)North

(3) After 15th Wave (4) After 22th Wave

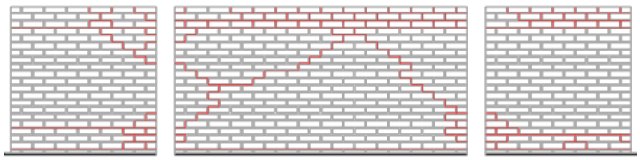

(5) After 23th Wave

Fig.3 – Crack patterns developed (Wall without Floor)

(1) Interior side (2)Exterior side at the corner of South and East

Photo 3 – Wall without Floor after the 23th Wave

The Measured accelerations, on the steel frame foundation (the point A20 of Fig. 2 and 4), at the top center of the central wall (A16) and at the middle center (A17), are in the loading direction (cm/s^2) which are shown in Table 1 and Table 2 as values divided by the gravitational acceleration g (= 980.665 (cm / s^2)).

Cracks in the wall without floor occurred after the 15 wave, occurred in the upper part of the right-hand side and the north wall of the lower part and the east wall of the 3 walls. After the 22 wave (Kobe-70%), the bricks at the top layer on the right side of the east wall and at the top layer in the north wall are falling down, and the measuring stopped. After the 23 wave, the diagonal cracks are generated in the south wall and the east wall, where the crack width is largely open, and the loading was completed (Photo 3).

Cracks in the wall with floor, after the 14 wave, occurred in the upper part of the three walls. After the 19 wave, the cracks in the top of the three walls are increased, and the diagonal cracks in the south wall also occurred.

Table 2 – Shaking Test Waves and Peaks of Measured Acceleration of Wall Specimen with Wire Netting with Floor

Shaking Test Waves (Shaking to 1 direction in horizontal and out-of-plane of the Central Wall)					Measured Acceleration (Shaking Direction)		
					Peak at	Peak at the Central Wall	
No.	Wave Type	Frequency (Hz)		Amp. (mm)	Steel Frame Foundation (g)	Upper and Center (g)	Middle and Center (g)
1	Sweep	0.8	20	0.5	0.01	0.06	0.06
2	Sweep	0.8	20	0.5	0.01	0.04	0.03
3	Random	5	20	0.5	0.03	0.09	0.08
4	Random	10	15	0.5	0.20	0.48	0.42
5	Random	10	15	2	0.28	0.98	0.57
6	Random	10	15	10	0.03	0.09	0.08
7	Random	10	15	15	0.33	1.29	1.09
8	Random	10	15	15	0.31	1.31	0.78
9	Random	10	15	20	0.33	1.86	1.78
10	Random	10	15	20	0.40	1.86	1.58
11	Random	10	15	30	0.32	2.13	2.39
12	Random	10	15	30	0.33	2.88	2.57
13	Random	10	15	40	0.48	3.11	2.82
14	Random	10	15	40	0.49	3.07	3.32
15	Random	10	15	50	0.40	2.43	2.83
16	Random	10	15	50	0.34	2.03	2.42
17	Random	5	15	30	0.54	3.86	3.89
18	Random	5	15	30	0.53	3.05	2.66
19	Random	5	15	40	0.64	5.04	3.64
20	Random	5	15	40	0.95	4.89	3.53
21	Random	5	15	50	0.44	1.16	0.85
22	Random	5	15	50	0.67	1.46	0.85
23	Random	5	10	30	0.84	2.14	1.53
24	Random	5	10	40	0.89	2.59	1.96
25	Random	5	10	50	1.67	4.58	2.43
26	Random	5	10	60	1.63	4.07	2.73
27	Random	5	10	70	1.67	4.58	2.43
28	Random	5	10	80	1.63	4.07	2.73

After the 23 wave, the cracks of the three wall's top are increased. At the 28wave, which amplitude is 80mm, because the diagonal cracks of the south wall and the north wall was wide open, the testing was completed (Photo 4).

To compare these 2 specimens with the specimens without wire netting in Ref. [1], the amplitude of the shaking waves when the brick is falling, was same or more. The peak value of the measured acceleration in the wall without floor in Ref. [1], on the steel foundation which is considered to be the input wave, is 1.18 (g), while the peak value of the same position in Table 1 is 2.22 (g) and it is more than the one of Ref. [1]. As for the wall with floor, on the steel foundation, the one of Ref. [1] is 2.11 (g) while the peak value of the same position of the Table 2 is 1.67 (g) and it is slightly less.

The width of cracks at the joints, compared with the wave before the bricks were falling down, was smaller than the case without wire netting (Fig. 3 and Fig. 5).

Therefore, by the wire netting, the effect of reducing the crack width occurring in the joint was obtained.

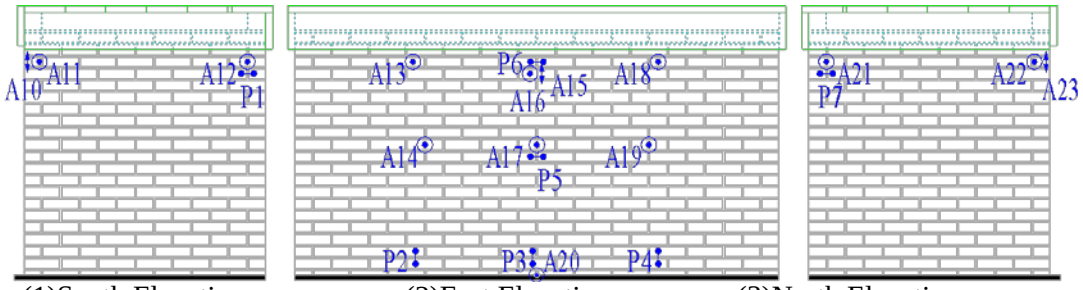

(1)South Elevation (2)East Elevation (3)North Elevation

(Note) : Accelerometers in the direction of out-of- plane
: Accelerometers in the direction of vertical
: PI gauges

Fig.4 – Instrumentation for the test (Wall with Floor)

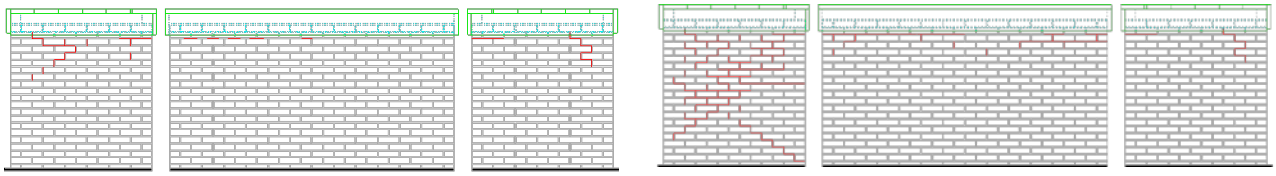

(i)South Elevation (ii)East Elevation (iii)North Elevation (i)South (ii)East (iii)North

(1) After 14th Wave (2) After 19th Wave

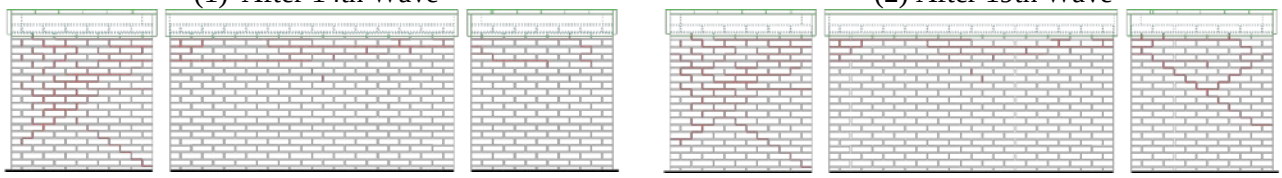

(i)South (ii)East (iii)North (i)South (ii)East (iii)North

(3) After 23th Wave (4) After 28th Wave

Fig.5 – Crack patterns developed (Wall with Floor)

(1) Interior side (2)Exterior side at the corner of South and East

Photo 4 – Wall with Floor after the 28th Wave

1.4 Predominant Frequency

In Fig. 6, the predominant frequency of the measured acceleration in each shaking test waves are shown from the point of the center and the middle of the central wall, and the point on the steel frame foundation. The predominant frequency of the center and the middle of the central wall seems a value close to the predominant frequency of the predominant frequency of the specimen or the predominant frequency on the steel foundation. As the waves proceed, it was reduced. By comparison of (1) and (2) in Fig. 6, the predominant frequency of the wall without floor is considered to be more than the wall with floor. Moreover, in the wall without floor, when the predominant frequency in the 3 wave was 31.6Hz, it decreased to 1.45Hz, in the 22 wave. On the wall with floor, the predominant frequency was 35.4Hz in the 1st wave, it was reduced to 9.51Hz in the 28 wave. And the predominant frequency of the two specimens of the experiment, when comparing the 2 specimens without the wire netting of Ref. [1], the predominant frequency of both of wall without floor and with floor are greater in slightly than the ones of the specimens without wire netting.

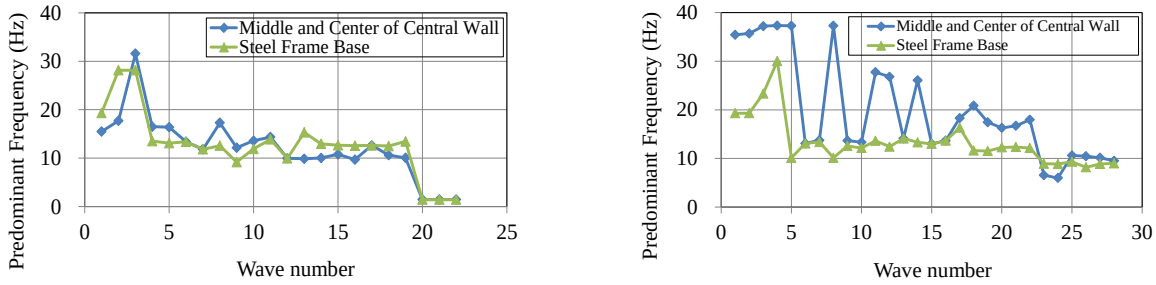

(1)Wall without Floor (2)Wall with Floor

Fig. 6 – The predominant frequency at Shaking Test Waves

1.5 Damping Factor

According to Ref. [2], in each period T of the frequency domain, the peak of the Fourier Amplitude of the absolute acceleration $\ddot{x}+\ddot{y}$ and the Fourier Amplitude of the recorded acceleration $\ddot{y}$ can give the maximum Response Amplification Ratio which is nearly equal to (1/(2h)) (Eq. (1)), where h is damping factor. Eq. (1) gives Eq. (2) and damping factor h .

$$\left(\frac{|\ddot{x}+\ddot{y}|_{\text{peak}}}{|\ddot{y}|}\right)_{\max} \fallingdotseq \frac{1}{2h} \tag{1}$$

$$h=\frac{1}{2}\cdot\left(\frac{|\ddot{y}|}{|\ddot{x}+\ddot{y}|_{\text{peak}}}\right)_{\min} \tag{2}$$

Where $\ddot{x}$: Response relative acceleration of SDOF or a recorded acceleration among A13～A19 in Fig. 2 or Fig. 4, $\ddot{y}$: Horizontal acceleration on ground or a recorded acceleration of A20.

Table 3 – Damping Factors h at Accelerometers

(1)Wall without Floor

Accelerometers No.	A13	A16	A18
h (%)	3.71	2.28	2.75
Accelerometers No.	A14	A17	A19
h (%)	5.28	2.97	4.05

(2)Wall with Floor

Accelerometers No.	A13	A16	A18
h (%)	4.15	2.95	5.54
Accelerometers No.	A14	A17	A19
h (%)	4.16	2.83	4.43

Table 3shows the damping factor *h* of each accelerometer during the 1st wave in Table 1 and Table2. The positions of the six accelerometers are shown in Fig. 2 or Fig. 4 for (A13, A14, A16, A17, A18 and A19). The period is about 0.028 seconds at the six points of the both of wall without and with floor.
According to Table 3, the *h* become the different values of the measurement positions. On the wall specimen without floor, the *h* are from 2.28 to 5.28 (%), and on the wall specimen with floor, the *h* are from 2.83 to 5.54 (%).

2. Response Values of Recent Acceleration Records

2.1 Introduction

Recent years, many earthquakes occurred and caused severe damage. In these earthquakes, many earthquake waves are recorded, for example, Kumamoto Earthquake, Japan in 2016 and Kathmandu of Nepal in 2015. These earthquake waves are very useful for the structural design of buildings. So, in this Section, the response values of recent acceleration records are analyzed succeeding to the Ref. [3].

2.2 Recent Acceleration Records

In Table 4, the earthquake waves adding to Ref. [3] are the main shock of 2016 Kumamoto Earthquake on 16 April 2016, [2004 Kawaguchi EW, Local Government] and [1995 Takatori NS, Japan Railroad].

Table 4 – Earthquake Waves for qCy* (= 0.2) adding to Ref. [3]

Earthquake Names [Earthquake Waves Names]	Direction	Peak Acceleration (cm/sec^2)	Epicentral distance (km)	Date and Time in Local Time	Remarks of Courtesy for Strong Motion Data
2016 Kumamoto Earthquake				16 April 2016. 01:25	
[20160416 Mashiki EW, L-Gov]	EW	825	6.4		L-Gov*1
[20160416 Mashiki EW2, KiK-net]	EW	653	7.3		KiK-net,*2
[20160416 Nishihara EW, L-Gov]	EW	770	15.8		L-Gov*1
2004 Niigata-ken Chuetsu Earthquake [2004 Kawaguchi EW, L-Gov]	EW	1676	2.8	23 Oct. 2004. 17:56	L-Gov*3
1995 Hyogo-ken Nanbu Earthquake [1995 Takatori NS, JR]	NS	606	11.3	17 Jan. 1995. 05:46	Japan Railroad

Notes) 1)qCy* : Design Shear Coefficient at Yielding Point referred to Section 2.3.
2)L-Gov*1 : Kumamoto Prefecture and Japan Meteorological Agency (JMA) in Ref. [4].
3)KiK-net*2 : Data of National Research Institute for Earth Science and Disaster Prevention in Ref. [5].
4)L-Gov*3 : Niigata Prefecture and JMA in Ref. [6].

In Table 5, the earthquake wave adding to Ref. [3] is 2015 Kathmandu Earthquake.

Table 5 – Earthquake Waves for qCy* (= 0.1) adding to Ref. [3]

Earthquake Names [Earthquake Waves Names]	Direction	Peak Acceleration (cm/sec^2)	Epicentral distance (km)	Date and Time in Local Time	Remarks of Courtesy for Strong Motion Data
2015 Kathmandu Earthquake [2015 KatNP NS, CESMD]	NS	160	59.9	25 April 2015. 11:56	CESMD*

Note) 1)CESMD* : Center for Engineering Strong Motion Data in Ref. [7].

2.3 Inelastic Dynamic Response Analysis Method

The response displacements of SDOF can help us to understand how much displacement took place in storeys of structures during earthquake.

Fig. 7 shows the hysteresis property of Tri-linear Model for the inelastic dynamic analysis. In this analysis, Takeda Model of Ref. [8] is applied which has the oriented point before the yielding point is the crack point in the opposite. The stiffness coefficient ${}_qk_4$ of unloading after the yielding point has some relationship with the stiffness ${}_qk_0$ between the yielding point and the crack point in the opposite side (${}_qk_4 = {}_qk_0(\delta y/\delta \text{peak})^{0.4}$).

The other parameters of qCc, ${}_qk_1$, ${}_qk_2$ and ${}_qk_3$ are calculated by equations in Figure 7. Equations of qCc=0.4·qCy and $({}_qk_2)=({}_qk_1)/3$ are referred to the Ref. [9].

The period T for each SDOF analysis is calculated by the mass m and the secant stiffness ky in Eq. (3).

$$T = 2\pi\sqrt{\frac{m}{ky}} = \frac{2\pi}{\sqrt{{}_qk_y \cdot g}} = 2\pi\sqrt{\frac{\delta y}{\text{qCy}\cdot g}} \tag{3}$$

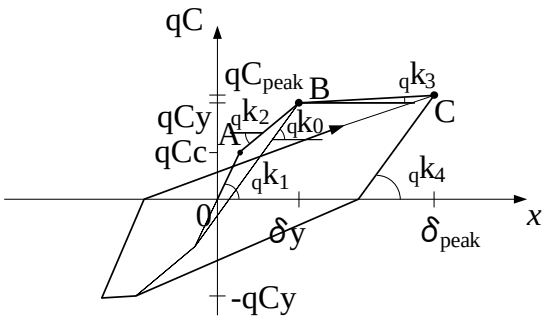

Notes)

(1) Takeda Model (The oriented point before the yield point is the cracking point in the opposite side.)
(2) The stiffness coefficient qko is the slope of a line joining the yield point in one direction to the cracking point in the other direction.
(3) The stiffness coefficient qk4 of unloading after the yield point is defined by the slope qko, δy and δpeak ; $${}_qk_4 = {}_qk_0\left(\frac{\delta y}{\delta \text{peak}}\right)^{0.4}$$
(4) Other parameters are referred to the Ref. [9].
(5) The shear coefficient of the cracking point qCc is 0.4 times of one of the yield point qCy ;. $$\text{qCc}=0.4\cdot\text{qCy}$$
(6) The initial stiffness coefficient qk1 is 2.2 times of the secant stiffness coefficient at the yield point ; $${}_qk_1 = 2.2\cdot\frac{\text{qCy}}{\delta y}$$
(7) The second stiffness coefficient qk2 is one third of qk1 ; $${}_qk_2 = \frac{{}_qk_1}{3}$$
(8) The third stiffness coefficient qk3 is one thousandth of the secant stiffness coefficient at the yield point ; $${}_qk_3 = \frac{1}{1000}\frac{\text{qCy}}{\delta y}$$
(9) The secant stiffness coefficient at the yield point qky is the division of the secant stiffness by the weight ; $${}_qk_y = \frac{\text{qCy}}{\delta y} = \frac{ky}{mg}$$
(10) Shear Coefficient qC is the division of the storey shear force by the weight ; $$\text{qC} = \frac{\text{Storey Shear Force (Q)}}{\text{Weight}\,(m\cdot g)}$$
(11) qCy : Shear Coefficient at the yield point of A (qCy = 0.1, 0.2.)
(12) qC_{peak} : Shear Coefficient at the peak of B
(13) Q : Storey Shear Force (kN) ($=k\cdot x$)
(14) ${}_qk_0$, ${}_qk_1$, ${}_qk_2$, ${}_qk_3$, ${}_qk_4$: Stiffness Coefficient (1/cm) ; $${}_qk_i = \frac{\text{Initial Stiffness } k_i}{\text{Weight}\,(m\cdot g)}$$
(15) h : Damping factor (= 0.05)
(16) g : Gravity Acceleration (=980 (cm/sec^2))

Fig. 7: Hysteresis property of Tri-linear Model

2.4 Analysis Results

According to Fig. 8, when the period *T* is less than 0.5 (sec), to be considered similar to the periods of low houses in wooden structures, steel structures or reinforced concrete structures, the maximum of inelastic response relative displacement is analyzed to be at most 23 (cm) of [20160416 Mashiki EW, L-Gov] and [20160416 Nishihara EW, L-Gov].

According to Fig. 9, when the period *T* is about 3.5 (sec), the maximum of inelastic response relative displacement is analyzed to be a maximum of [2015 KathNP NS, CESMD]. This value is still increasing to more than 3 (m) when the period is more than 3.5 (sec) while the response ductility is less than 1.2 (-).

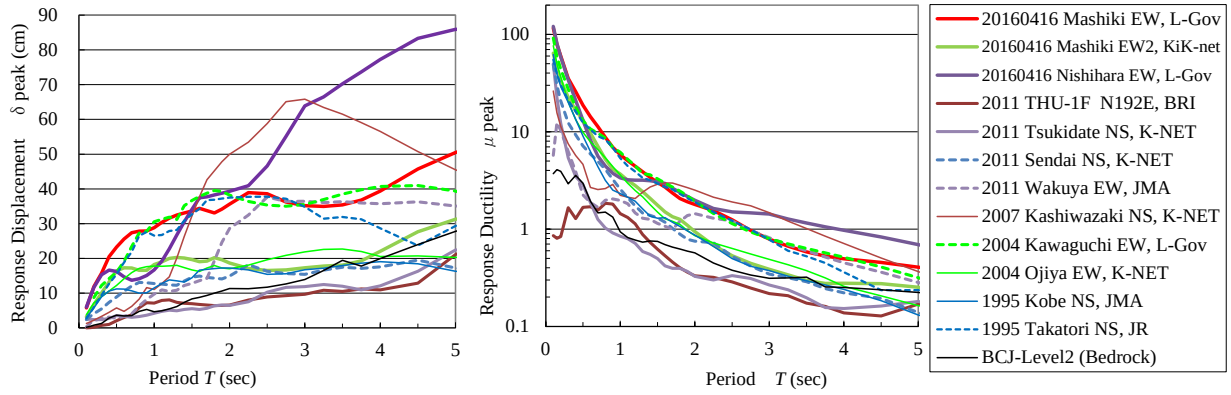

(1) Response Displacement Spectra (2) Response Ductility Spectra

Fig. 8 – Inelastic Response Spectra (qCy=0.2, *h* =0.05)

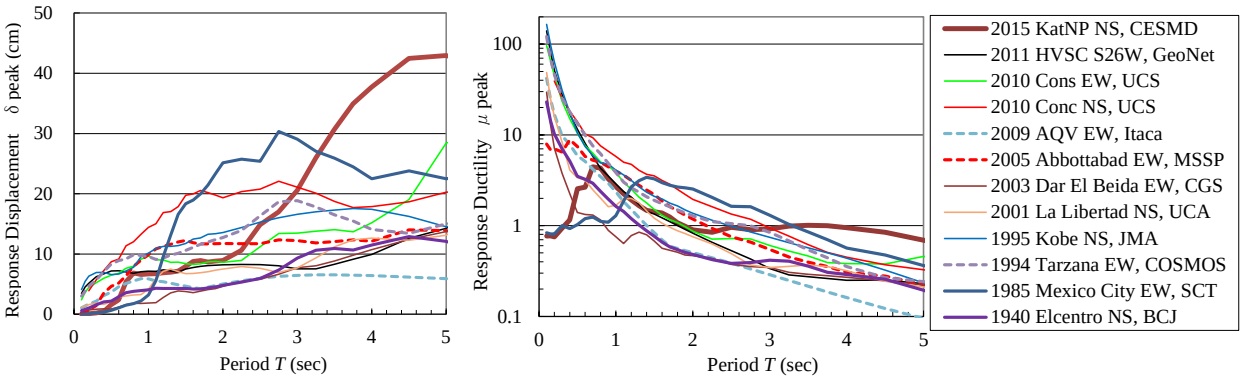

(1) Response Displacement Spectra (2) Response Ductility Spectra

Fig. 9 – Inelastic Response Spectra (qCy=0.1, *h* =0.05)

3. Summary

(1) Out-of-plane Dynamic Test of Unreinforced Masonry Walls Retrofitted by wire netting was executed in shaking table. The amplitudes of shaking test waves are similar or more than the one of masonry walls without wire netting.

(2) The predominant frequency indicates a value close to the one of the specimens or the one on the steel foundation. As the shaking test waves proceed, they are reduced.

(3) When the wire netting are put on the wall inside, the effect of reducing the crack width in the joints of the wall is obtained.

(4) According to the out-of-plane test of unreinforced masonry walls, the damping factors are different in the recorded points which are 2-5%.

(5) Response values of recent acceleration records are analyzed when the shear coefficient at the yielding point of the Tri-linear Model is 0.1 and 0.2.

4. References

[1] Taiki Saito, Luis Moya, Cesar Fajardo and Koichi Morita. : Experimental Study on Dynamic Behavior of Unreinforced Masonry Walls, Journal of Disaster Research Vol.8 No.2, 2013, pp.305-311.

[2] Inukai M, Azuhata T, Saito T, Morita K, Tani M, Noguchi K, (2015): Experimental Study on Out-of-Plane Tests of Unreinforced Masonry Walls Retrofitted and Damping Factor. *Proceedings of the 11th Annual Meeting of Japan Association for Earthquake Engineering, CD, pp.1-7*, Tokyo, Japan. (in Japanese)

[3] Inukai M, Kashima T, Saito T (2014): Response Values in Hysteresis Properties by Acceleration Records. *Usb of 2ECEES (The Second European Conference on Earthquake Engineering and Seismology)*, No. 227, Istanbul, Turkey.

[4] Japan Meteorological Agency (JMA) Homepage: Strong Motion Data of Kumamoto Earthquake on 01:25, 16 April 2016, Local Government and JMA, http://www.data.jma.go.jp/svd/eqev/data/kyoshin/jishin/1604160125_kumamoto/index2.html (in Japanese).

[5] Kyoshin Network K-NET Homepage: http://www.kyoshin.bosai.go.jp/kyoshin/quake/index_en.html, National Research Institute for Earth Science and Disaster Resilience, Japan.

[6] JMA Homepage: Strong Motion Data of Niigata-ken Chuetsu Earthquake on 17:56, 23 Oct. 2004, Local Government and JMA, http://www.data.jma.go.jp/svd/eqev/data/kyoshin/jishin/041023_niigata/nigata_main.htm (in Japanese).

[7] Center for Engineering Strong Motion Data Homepage: Lamjung, Nepal Earthquake of 25 April 2015, http://www.strongmotioncenter.org/cgi-bin/CESMD/selectpage.pl?Lamjung_us20002926%2FNPKATNP=on&Raw=on

[8] Takeda T., Sozen M.A, et al.: Reinforced Concrete Response to Simulated Earthquakes, Proceeding ASCE Vol. 96, NO ST-12, December 1970, pp.2557-2573

[9] Inukai M, Kashima T, Saito T, Azuhata T (2015): Predominant Periods of Multi-Degree-of-Freedom System Analysis and Dynamic Soil-Structure Interaction for Building Structures. *Proceedings of the VI International Conference on Coupled Problems in Science and Engineering*, International Center for Numerical Methods in Engineering (CIMNE), Ebook, pp.278-289, Venice, Italy.